On-chip CMOS compatible reconfigurable optical delay line with separate carrier tuning for microwave photonic signal processing

Maurizio Burla,[1,*] **David Marpaung,**[1] **Leimeng Zhuang,**[1] **Chris Roeloffzen,**[1] **Muhammad Rezaul Khan,**[1] **Arne Leinse,**[2] **Marcel Hoekman,**[2] **and René Heideman**[2]

[1]*Telecommunication Engineering Group, Faculty of Electrical Engineering, Mathematics and Computer Science, University of Twente, Enschede, The Netherlands*
[2]*LioniX BV, Enschede, The Netherlands*
*m.burla@ewi.utwente.nl

Abstract: We report, for the first time, an integrated photonic signal processor consisting of a reconfigurable optical delay line (ODL) with a separate carrier tuning (SCT) unit and an optical sideband filter on a single CMOS compatible photonic chip. The processing functionalities are carried out with optical ring resonators as building blocks. We show that the integrated approach together with the use of SCT technique allows the implementation of a wideband, fully-tunable ODL with reduced complexity. To highlight the functionalities of the processor, we demonstrate a reconfigurable microwave photonic filter where the ODL has been configured in a bandwidth over 1 GHz.

OCIS codes: (070.1170) Analog optical signal processing; (130.3120) Integrated optics devices; (250.5300) Photonic integrated circuits; (230.5750) Resonators.

References and links

1. J. Capmany and D. Novak, "Microwave photonics combines two worlds," Nat. Photonics **1**(6), 319-330 (2007).
2. J. Yao, "Microwave photonics," J. Lightwave Technol. **27**(3), 314-335 (2009).
3. A. Seeds, "Microwave photonics," IEEE Trans. Microw. Theory Tech. **50**(3), 877-887 (2002).
4. J. Capmany, B. Ortega, D. Pastor, and S. Sales, "Discrete-time optical processing of microwave signals," J. Lightwave Technol. **23**(2), 702-723 (2005).
5. M. H. Khan, H. Shen, Y. Xuan, L. Zhao, S. Xiao, D. E. Leaird, A. M. Weiner, and M. Qi, "Ultrabroad-bandwidth arbitrary radiofrequency waveform generation with a silicon photonic chip-based spectral shaper," Nat. Photonics **2**(4), 117–122 (2010).
6. A. Meijerink, C. G. H. Roeloffzen, R. Meijerink, Z. Leimeng, D. A. I. Marpaung, M. J. Bentum, M. Burla, J. Verpoorte, P. Jorna, A. Hulzinga, and W. van Etten, "Novel ring resonator-based integrated photonic beamformer for broadband phased array receive antennas—Part I: design and performance analysis," J. Lightwave Technol. **28**(1), 3–18 (2010).
7. L. Zhuang, C. G. H. Roeloffzen, A. Meijerink, M. Burla, D. A. I. Marpaung, A. Leinse, M. Hoekman, R. G. Heideman, and W. van Etten, "Novel ring resonator-based integrated photonic beamformer for broadband phased array receive antennas—Part II: experimental prototype," J. Lightwave Technol. **28**(1), 19–31 (2010).
8. Y. Huo, S. Sandhu, J. Pan, N. Stuhrmann, M. L. Povinelli, J. M. Kahn, J. S. Harris, M. M. Fejer, and S. Fan, "Experimental demonstration of two methods for controlling the group delay in a system with photonic-crystal resonators coupled to a waveguide," Opt. Lett. **8**(36), 1482–1484 (2011).
9. W. Xue, S. Sales, J. Capmany, and J. Mørk, "Wideband 360 degrees microwave photonic phase shifter based on slow light in semiconductor optical amplifiers," Opt. Express **6**(18), 6156–6163 (2010).

#153078 - $15.00 USD Received 18 Aug 2011; revised 4 Oct 2011; accepted 4 Oct 2011; published 17 Oct 2011

10. Y. Chen, W. Xue, F. Ohman, and J. Mørk, "Theory of optical-filtering enhanced slow and fast light effects in semiconductor optical waveguides," J. Lightwave Technol. **23**(26), 3734–3743 (2008).
11. S. Sales, W. Xue, J. Mørk, and I. Gasulla, "Slow and fast light effects and their applications to microwave photonics using semiconductor optical amplifiers," IEEE Trans. Microw. Theory Tech. **11**(58), 3022–3038 (2010).
12. L. Thévenaz, "Slow and fast light in optical fibers," Nat. Photonics **2**(8), 474–481 (2008).
13. S. Chin, L. Thévenaz, J. Sancho, S. Sales, J. Capmany, P. Berger, J. Bourderionnet, and D. Dolfi, "Broadband true time delay for microwave signal processing, using slow light based on stimulated Brillouin scattering in optical fibers," Opt. Express **18**(21), 22599–22613 (2010).
14. J. Sancho, S. Chin, M. Sagues, A. Loayssa, J. Lloret, I. Gasulla, S. Sales, L. Thévenaz, and J. Capmany, "Dynamic microwave photonic filter using separate carrier tuning based on stimulated Brillouin scattering in fibers," IEEE Photon. Technol. Lett. **22**(23), 1753–1755 (2010).
15. M. S. Rasras, C. K. Madsen, M. A. Cappuzzo, E. Chen, L. T. Gomez, E. J. Laskowski, A. Griffin, A. Wong-Foy, A. Gasparyan, A. Kasper, J. Le Grange, and S. S. Patel, "Integrated resonance-enhanced variable optical delay lines," IEEE Photon. Technol. Lett. **17**(4), 834–836 (2005).
16. L. Zhuang, C. G. H. Roeloffzen, R. G. Heideman, A. Borreman, A. Meijerink, and W. van Etten, "Single-chip ring resonator-based 1×8 optical beam forming network in CMOS-compatible waveguide technology," IEEE Photon. Technol. Lett. **15**(19), 1130–1132 (2007).
17. F. Morichetti, A. Melloni, A. Breda, A. Canciamilla, C. Ferrari, and M. Martinelli, "A reconfigurable architecture for continuously variable optical slow-wave delay lines," Opt. Express **25**(15), 17273–17282 (2007).
18. J. Cardenas, M. A. Foster, N. Sherwood-Droz, C. B. Poitras, H. L. R. Lira, B. Zhang, A. L. Gaeta, J. B. Khurgin, P. Morton, and M. Lipson, "Wide-bandwidth continuously tunable optical delay line using silicon microring resonators," Opt. Express **25**(18), 26525–26534 (2010).
19. P. A. Morton and J. B. Khurgin, "Microwave photonic delay line with separate tuning of the optical carrier," IEEE Photon. Technol. Lett. **21**(22), 1686–1688 (2009).
20. J. Cardenas, S. Manipatruni, N. Sherwood-Droz, C. B. Poitras, B. Zhang, J. B. Khurgin, P. A. Morton, and M. Lipson, "Large tunable delay of an RF photonic signal with 130 GHz bandwidth using silicon microresonators," in *Conference on Lasers and Electro-Optics*, OSA Technical Digest (CD) (Optical Society of America, 2010), paper CWG3.
21. M. Pu, L. Liu, W. Xue, Y. Ding, L. H. Frandsen, H. Ou, K. Yvind, and J. M. Hvam, "Tunable microwave phase shifter based on silicon-on-insulator microring resonator," IEEE Photon. Technol. Lett. **22**(12), 869–871 (2010).
22. F. Morichetti, A. Melloni, M. Martinelli, R. G. Heideman, A. Leinse, D. H. Geuzebroek, and A. Borreman, "Box-shaped dielectric waveguides: a new concept in integrated optics?," J. Lightw. Technol. **25**(9), 2579-2589 (2007).
23. K. Daikoku and A. Sugimura, "Direct measurement of wavelength dispersion in optical fibres-difference method," Elec. Letters **14**(5), 149–151(1978).
24. A. Loayssa and F. J. Lahoz, "Broad-band RF photonic phase-shifter based on stimulated Brillouin scattering and single-sideband modulation," IEEE Photon. Technol. Lett. **18**(1), 208-210 (2006).
25. J. Lloret, J. Sancho, M. Pu, I. Gasulla, K. Yvind, S. Sales, and J. Capmany, "Tunable complex-valued multitap microwave photonic filter based on single silicon-on-insulator microring resonator," Opt. Express **19**(13), 12402–12407 (2011).
26. A. Loayssa, J. Capmany, M. Sagues, and J. Mora, "Demonstration of incoherent microwave photonic filters with all-optical complex coefficients," IEEE Photon. Technol. Lett. **18**(13–16), 1744–1746 (2006).
27. W. Li, N. H. Zhu, L. X. Wang, J. S. Wang, J. G. Liu, Y. Liu, X. Q. Qi, L. Xie, W. Chen, X. Wang, and W. Han, "True-time delay line with separate carrier tuning using dual-parallel MZM and stimulated Brillouin scattering-induced slow light," Opt. Express **19**(13), 12312–12324 (2011).

1. Introduction

Reconfigurable optical delay lines (ODL) and wideband tunable phase shifters have primary importance in a number of microwave photonic (MWP) signal processing applications like filtering [1–4], arbitrary waveform generation [5] or control of wideband phased-array antennas [6, 7]. Various approaches have been proposed to implement reconfigurable true time delay (TTD) lines employing photonic crystals [8], semiconductor waveguides [9–11] or exploiting nonlinear effects in optical fibers, such as the stimulated Brillouin scattering (SBS) [12–14]. Moreover, cascaded optical ring resonators have also been considered to provide tunable time delay [15–18]. The main advantages of this approach are the continuous tunability with large instantaneous bandwidth, compactness and CMOS compatibility of the technology.

Many solutions, however, suffer a tradeoff between maximum achievable delay, operating frequency and bandwidth. For MWP signal processing schemes like filtering or beamforming

#153078 - $15.00 USD Received 18 Aug 2011; revised 4 Oct 2011; accepted 4 Oct 2011; published 17 Oct 2011

it is advantageous to employ a single sideband with carrier (OSSB+C) modulation scheme to limit the delay bandwidth [13, 19] without resorting to coherent detection scheme where the optical carrier is completely removed. Thus, in this scheme, one would employ a delay line that imposes a linear phase response over the whole frequency range comprised between the optical carrier and the highest frequency component of the RF sideband (shown as the dashed line in Fig. 1). In this case the delay bandwidth, defined as the frequency range where the linear phase response of the ODL is obtained, depends strongly on the absolute frequency of the RF signal. The separate carrier tuning (SCT) technique [13–14, 19–20] can be used to relax this stringent requirement on the ODL. In this scheme, basically, the ODL would impose a linear phase response over the RF sideband only. As for the optical carrier, a separate component is used to apply the correct phase shift as it would experience when an ideal delay unit with a linear phase slope over the whole frequency range is employed (Fig. 1). With this scheme, the delay bandwidth of the ODL is independent of the absolute RF frequency. In this work we propose and experimentally demonstrate a scheme where the ODL, the SCT and the optical sideband filter (OSBF) necessary to create the OSSB+C spectrum are integrated in a single CMOS compatible photonic chip. This approach brings advantages in terms of compactness together with wideband performance and full tunability. The functionality in terms of full-2π carrier phase shift and continuously tunable delay is demonstrated by implementing a reconfigurable 2-tap complex-coefficients microwave photonic notch filter.

2. Theory of separate carrier tuning

Let us consider an OSSB+C modulation where only the upper sideband is kept, as in Fig. 1.

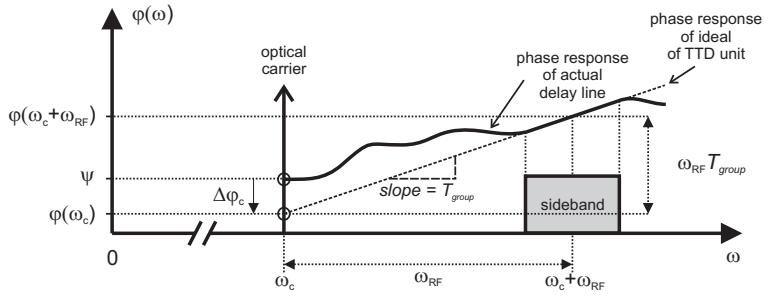

Fig. 1. Principle of operation of an optical true time delay unit with separate carrier tuning.

The group delay T_{group} applied to the signal at frequency $\omega_{\text{c}} + \omega_{\text{RF}}$ is given by the slope of the optical phase characteristic at the same frequency:

$$T_{\text{group}} = \left.\frac{\partial \varphi(\omega)}{\partial \omega}\right|_{\omega_{\text{c}}+\omega_{\text{RF}}} \tag{1}$$

For TTD operation, the RF phase should be a linear function of frequency over the whole frequency range [19], with the slope T_{group}. The desired carrier phase should then be

$$\varphi(\omega_{\text{c}}) = \varphi(\omega_{\text{c}} + \omega_{\text{RF}}) - \omega_{\text{RF}} \left.\frac{\partial \varphi(\omega)}{\partial \omega}\right|_{\omega_{\text{c}}+\omega_{\text{RF}}} \tag{2}$$

If a dispersive device is used to add a constant phase slope to the sideband, as in Eq. (1), the carrier phase will assume a certain value ψ, which can deviate from the desired phase $\varphi(\omega_{\text{c}})$, as illustrated in Fig. 1. Based on the separate carrier tuning approach, to achieve TTD operation,

#153078 - $15.00 USD Received 18 Aug 2011; revised 4 Oct 2011; accepted 4 Oct 2011; published 17 Oct 2011

the carrier phase should be adjusted to the value given by Eq. (2), by adding a phase shift to the carrier equal to

$$\Delta\varphi_c = \varphi(\omega_c) - \psi \tag{3}$$

It should be kept in mind that the carrier phase adjustment should be applied modulus of 2π since the carrier is monochromatic. The details on SCT technique applied to delay lines based on SBS in optical fibers can be found in [13].

3. Principle of operation and device realization

The schematic of the MWP processor consisting of the OSBF, the reconfigurable ODL and the SCT unit is depicted in Fig. 2. The OSBF is a Mach-Zehnder interferometer loaded with an optical ring resonator in one of its arms (i.e. MZI + ring type) (Fig. 2(a)).

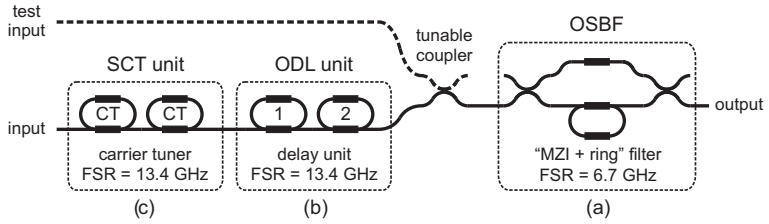

Fig. 2. Schematic of the delay structure employed to demonstrate the single-chip SCT-based optical delay line: (a) optical sideband filter (OSBF); (b) optical delay line (ODL) unit; (c) separate carrier tuning (SCT) unit.

The OSBF is used to remove one of the RF sidebands (in this case the lower sideband) of a double sideband with carrier (DSB+C) modulation signal generated from an intensity modulation of the optical carrier. The DSB+C spectrum and the magnitude response of the OSBF is depicted in Fig. 3(a). The detail of the OSBF design has been reported elsewhere [6].

The reconfigurable ODL consists a pair of cascaded all-pass ORRs [15] as shown in Fig. 2(b). These ORRs can be tuned in such a way to approximate a linear phase response over the sideband, with the specific slope Eq. (1) that gives the desired group delay T_{group}. The desired phase response is shown in Fig. 3(b).

The SCT unit is implemented using a pair of cascaded ORRs, exploiting the dispersive phase response of the resonator [19,21]. This is characterized by a 2π optical phase transition centered at the resonant wavelength. The separate tuning is thus obtained by tuning the phase transition of an ORR and then simply adjusting the position of its resonant frequency with respect to the carrier wavelength (see Fig. 3(c)). This approach was demonstrated in [21] where an RF phase shift up to 336° was obtained employing a tunable silicon-on-insulator (SOI) microring resonator (MRR). Nonetheless, this solution may require a detuning of the resonance of the MRR in the order of several GHz. Here we use two optical ring resonators, as shown in Fig. 2(c), in order to achieve a sharper transition in the phase transfer around the resonance frequency, as visible in Fig. 3(c). This permits to give a complete 360° phase shift to the carrier with moderate detuning of the resonant frequency, thus limiting the dispersion effects only in the vicinity of the desired wavelength, without sensibly affecting the linear phase transfer desired in the spectral region occupied by the sideband (Fig. 3(c)). In addition to that, using two ORRs allows to keep a relatively low quality factor for the resonators, thus minimizing their insertion loss.

The structure in Fig. 2 is realized in a low-loss CMOS compatible TriPleX™ waveguide technology [22]. The realized ORRs have a free spectral range of 13.4 GHz and the OSBF has an FSR of 6.7 GHz. The ORRs and the OSBF are fully tunable using thermo-optical tuning

#153078 - $15.00 USD Received 18 Aug 2011; revised 4 Oct 2011; accepted 4 Oct 2011; published 17 Oct 2011

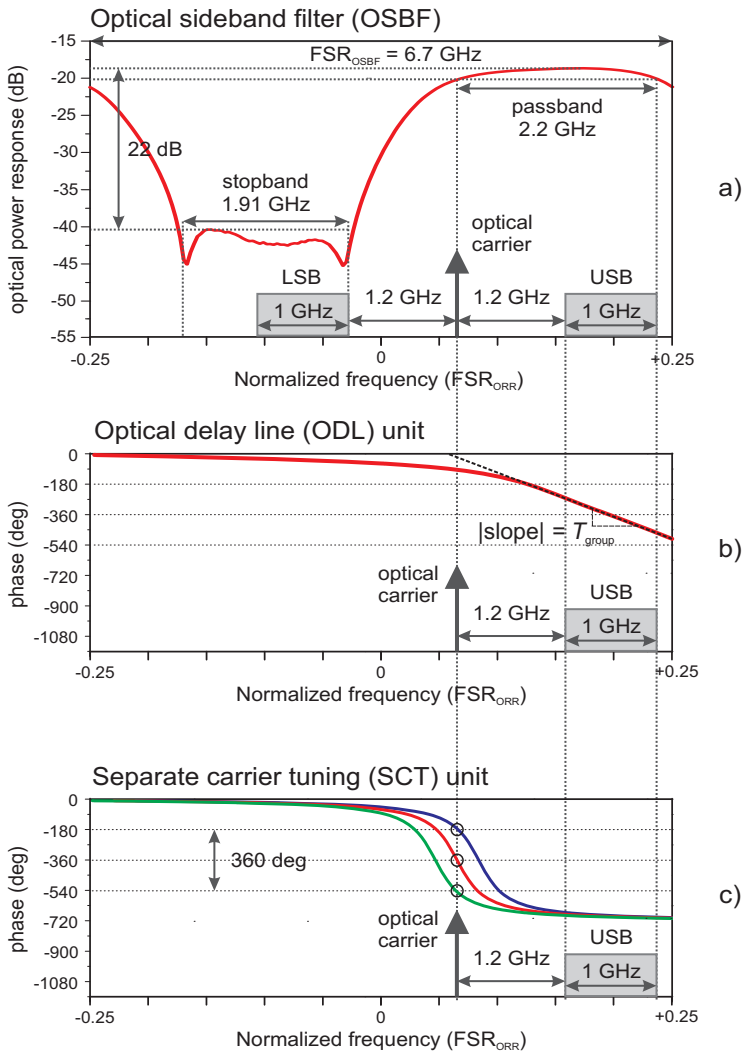

Fig. 3. Measured frequency response of subsection (a) and simulated responses of subsections (b) and (c) of the optical delay line, over one FSR of the OSBF (6.7 GHz).

with chromium heaters that have been deposited on the optical chip. Using these heaters, the ORRs can be fully tuned in terms of their resonance frequencies and their Q-factors as will be explained in the next section.

4. Experiment

The measurement setup in Fig. 4 is used to analyze the performance of the OSBF, the ODL and the SCT sections. We use a DFB laser with an optical power of 100 mW (EM4 Inc.), a Mach-Zehnder modulator (MZM, Avanex FA20), an erbium-doped fiber amplifier (EDFA) and a 10 GHz photodetector (PD, Discovery Semiconductor DSC 710). A vector network analyzer (VNA, Agilent N5230) is used for the amplitude and phase transfer measurements; the optical responses can be displayed on the VNA by using the phase shift method [23], which is a similar method to the one implemented in a lightwave component analyzer [8].

#153078 - $15.00 USD Received 18 Aug 2011; revised 4 Oct 2011; accepted 4 Oct 2011; published 17 Oct 2011

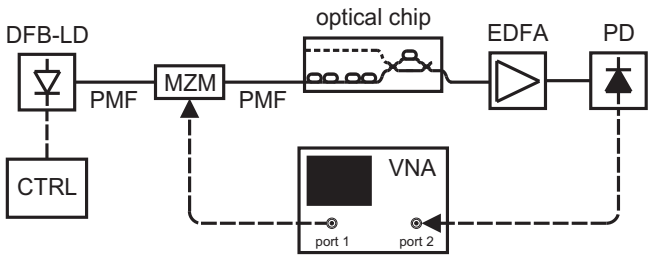

Fig. 4. Schematic of the measurement setup. Polarization maintaining optical fibers (PMF) are used for the interconnection of laser, modulator and optical chip.

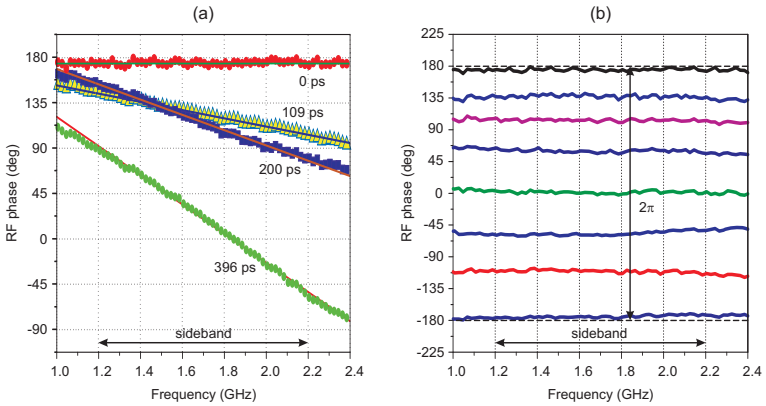

Fig. 5. (a) Measured (symbols) and theoretical (solid lines) phase responses over the signal sideband. Different slopes (corresponding to different delays) can be set using the ODL unit. (b) Phase shift of the RF phase responses. A phase shift over 2π is achieved by changing the phase of the optical carrier employing the SCT unit. The constant slope for all traces shows that the amount of delay is not influenced by the carrier tuning.

Figure 3(a) shows the measured magnitude response of the OSBF, in comparison with a schematic representation of the DSB+C signal spectrum to be processed. Assuming an optical suppression of at least 22 dB for the undesired sideband, the usable bandwidth in which it is possible to achieve OSSB+C modulation for the RF signal is between 1.2 GHz and 2.2 GHz as illustrated in Fig. 3(a).

In Fig. 5 we show how the integrated delay line can be used to provide different values of group delay to the signal sideband (visible as different slopes of the phase response, Fig. 5(a)) and arbitrary phase shifting to the optical carrier (Fig. 5(b)).

The amount of time delay (i.e. the slope of the phase response) of the ODL unit can be varied with continuity by means of tuning the resonance frequencies and the coupling factor (hence the Q-factor) of the ORRs in Fig. 2(b). By properly cascading the ORRs (i.e. adding their group delay response) in principle a large and wideband true time delay can be achieved. The detail of this principle is reported in [7, 16]. The phase responses obtained with the ODL are displayed in Fig. 5(a), and show good agreement with their theoretical responses. In the measurements, the electrical delay function of the VNA has been employed to compensate for the additional group delay given by the transmission path external to the tunable ODL (e.g. coax. cables, fibers, EDFA), in such a way that the slope of the phase response in Fig. 5(a) would represent the delay provided by the integrated ODL only.

In order to demonstrate the effectiveness of the SCT unit, in Fig. 5(b) we show measured RF

#153078 - $15.00 USD Received 18 Aug 2011; revised 4 Oct 2011; accepted 4 Oct 2011; published 17 Oct 2011

phase characteristics on the detected sideband when a variable phase shift (PS) between 0 and 2π is imposed to the optical carrier via the ORRs of the CT unit in Fig. 2(c). In a OSSB+C modulation scheme, the phase shift imparted on the optical carrier generates an equal phase shift on the detected electrical signal, constant with respect to RF frequency [24]. This effect is visible in Fig. 5(b), where the constant phase shift over the detected sideband shows that the carrier phase is effectively being shifted over the whole 2π range, and the fact that the slope does not change confirms that the carrier phase can be tuned without affecting the linear phase response at the delay band as suggested in Fig. 3.

5. Microwave photonic filter demonstration

To demonstrate the functionality of the delay line when employed in a specific application, we built a 2-tap reconfigurable microwave photonic filter (MPF) with complex coefficients. For 2-taps, the general expression of the transfer function [4, 13, 25–27] reduces to

$$H(\omega) = a_0 + a_1 e^{-j\omega T} \tag{4}$$

where ω is the microwave frequency, $a_0 = |a_0|e^{-j0}$, $a_1 = |a_1|e^{-j\varphi}$ are the real and the complex tap coefficients, respectively, T is the basic delay of the MPF and φ the phase difference between the taps. In this demonstration we use the ODL unit to change the MPF basic delay and the SCT unit to adjust the φ, thereby fully reconfiguring the MPF response.

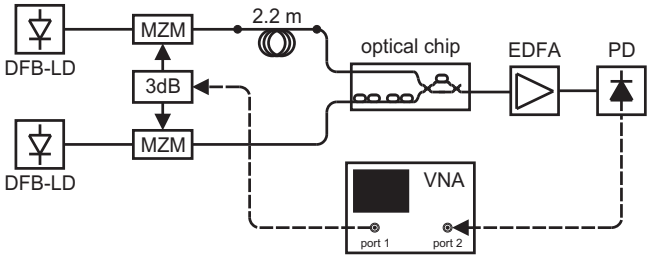

Fig. 6. Schematic of the 2-tap microwave photonic filter.

The schematic of the incoherent MPF is shown in Fig. 6. The optical frequencies were generated using two DFB laser diodes (DFB-LDs). The laser wavelengths have been set to have an offset over 1 nm (corresponding to approximately 125 GHz of frequency difference between the DFB-LDs) to prevent that a possible beating frequency might fall in the passband of the photodetector and create signal distortions. The two taps have a length imbalance of 2.2 m, which gives a delay difference of approximately 10.68 ns and free-spectral range of 93.6 MHz. One signal tap propagates through the ODL while the other one enters the chip from the OSBF test input port, thereby bypassing the ODL and the SCT. These taps are combined using a tunable coupler prior to entering the OSBF, as depicted in Fig. 2. In this way, if desired, a single OSBF can be used to suppress the lower sideband for both taps. This is possible by exploiting the periodic response of the integrated OSBF, by simply setting the frequency spacing between the carrier wavelenghts to be a multiple of the FSR of the OSBF. The filter taps amplitudes a_0 and a_1 can be equalized by modifying the coupling ratio of the tunable coupler.

By operating the SCT unit and the ODL, as in Fig. 7, the notch positions and the FSR of the MPF can be tuned independently. In particular, Fig. 7(a) shows how the MPF notch positions can be shifted by 360 degrees by operating the SCT unit in Fig. 2(c). A 100% tunability can be achieved, as expected from the the phase shift capability of the ODL shown in Fig. 5(b). The equal shape of the individual responses and their constant FSR demonstrates that the carrier

#153078 - $15.00 USD Received 18 Aug 2011; revised 4 Oct 2011; accepted 4 Oct 2011; published 17 Oct 2011

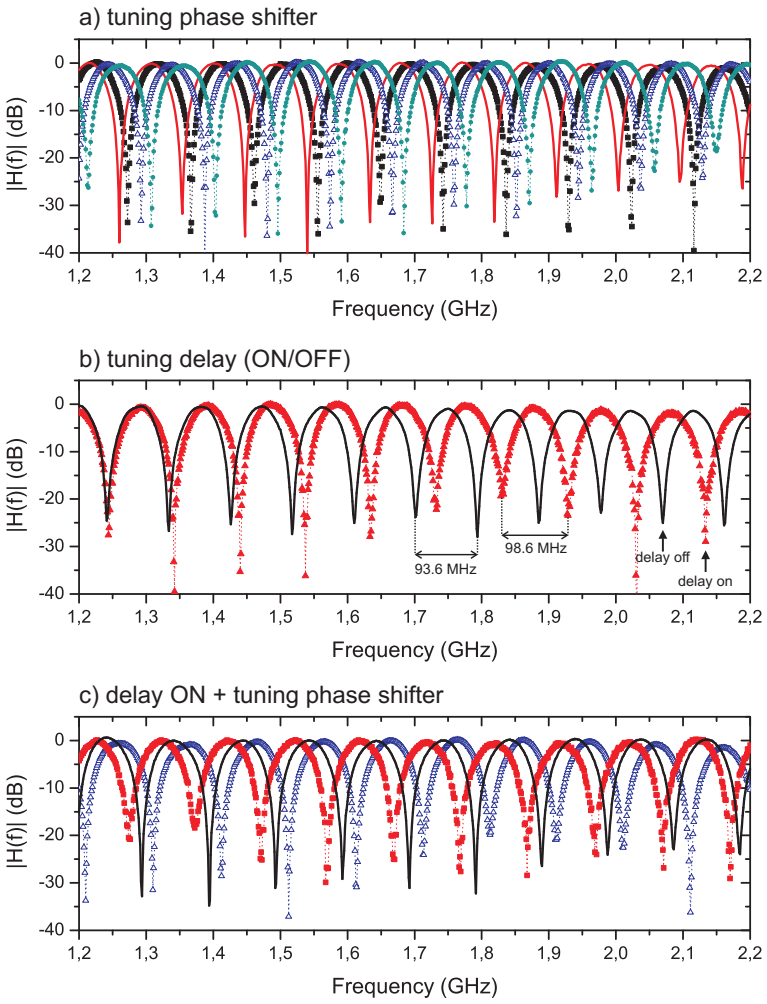

Fig. 7. Measured magnitude responses of the MPF. A continuous 100% fractional tuning can be achieved by the SCT unit, without changing the FSR (a). The FSR can be changed from 93.6 MHz to 98.6 MHz by setting the tunable delay to 540 ps (b). The fact that the FSR of the MPF does not vary when shifting the response, shows that operating the carrier tuner does not disrupt the delay response imposed over the sideband by the delay unit (c).

phase tuning does not influence neither the amplitude nor the delay in the passband, as expected from the principle of operation of the SCT unit represented in Fig. 3(c).

Figure 7(b) shows the capability the ODL to impose a tunable group delay over the entire sideband. The solid line represents the MPF response when no delay is applied to the tunable tap (0 ps line in Fig. 5(a)). This condition is indicated as “delay off”. The dotted line shows how the response is modified when a group delay of approximately 540 ps is set in the ODL (“delay on”). The application of this amount of delay reduces the basic delay T of the MPF from 10.68 ns to 10.14 ns, with a corresponding increase the FSR from 93.6 MHz to 98.6 MHz.

In Fig. 7(c) different measured MPF responses are reported, when both the ODL and the SCT units are active simultaneously. As described before, here the ODL has been kept on the “delay on” condition in all traces. It is possible to see that the FSR keeps to the 98.6 MHz value,

#153078 - $15.00 USD Received 18 Aug 2011; revised 4 Oct 2011; accepted 4 Oct 2011; published 17 Oct 2011

independently by the absolute position of the MPF notches, which can be set applying a phase shift to the carrier via the SCT section as in Fig. 7(a). This latter measurement confirms that the SCT section can be operated without affecting the amount of delay in the ODL section.

6. Conclusion

We have experimentally demonstrated a reconfigurable ODL based on the SCT technique where, for the first time, all the required components are integrated on a single photonic chip. The functionality was demonstrated over a bandwidth in excess of 1 GHz by employing the ODL to fully reconfigure the response of a 2-tap complex-valued MPF. The operating bandwidth can be readily extended just by adding more ORRs in the delay section of the ODL and simply increasing the FSR of the OSBF by design.

The ODL proposed here opens a path towards the implementation of a wideband and fully reconfigurable MPF with multiple taps monolithically integrated on a single chip. The number of taps can be increased by multiplying the delay sections and SCT units, while sharing a single OSBF. A schematic of a possible implementation is shown in Fig. 8.

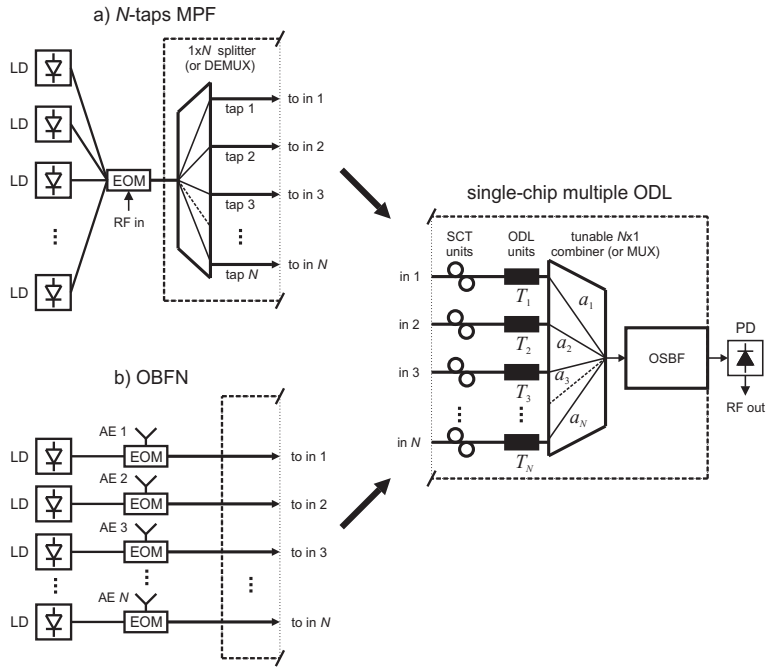

Fig. 8. Schematic example of a multiple optical delay line (right). This structure could be used, for example, to implement (a) an incoherent multitap microwave photonic filter with complex coefficients, or (b) an optical beamforming network (OBFN) for phased array antennas.

Notably, the same multiple ODL structure could also be operated as an integrated optical beamforming network (OBFN) for the control of phased array antenna systems, according to the schematic displayed in Fig. 8(b). In this case, the individual delay lines are used to give the desired time difference to the RF signals originating from the individual antenna elements (AE) of the array. This OBFN could use multiple laser sources, each of them acting as a carrier for the RF signal originated from a different antenna element.

#153078 - $15.00 USD Received 18 Aug 2011; revised 4 Oct 2011; accepted 4 Oct 2011; published 17 Oct 2011

Acknowledgments

This work was supported by funding within the framework of the MEMPHIS project, for which the authors gratefully acknowledge the support of the Smart Mix Programme of the Netherlands Ministry of Economic Affairs and the Netherlands Ministry of Education, Culture and Science.

#153078 - $15.00 USD Received 18 Aug 2011; revised 4 Oct 2011; accepted 4 Oct 2011; published 17 Oct 2011